DMD Fast Forward. Published on December 19, 2018 as DOI: 10.1124/dmd.118.084525
This article has not been copyedited and formatted. The final version may differ from this version.

Characterization of anacetrapib distribution into the lipid droplet of adipose tissue in mice and human cultured adipocytes

Douglas G. Johns, Lauretta LeVoci, Mihajlo Krsmanovic, Min Lu, Georgy Hartmann, Suoyu Xu, Sheng-Ping Wang, Ying Chen, Thomas Bateman, Robert O. Blaustein.

Merck & Co., Inc., Kenilworth, NJ, USA

Author affiliations:

DJ: Department of Translational Pharmacology

LL, MK, ML, SPW, YC: Department of Cardiometabolic Disease/Atherosclerosis

GH, SX, TB: Department of Pharmacokinetics, Pharmacodynamics and Drug Metabolism

ROB: Clinical Research.

Running title: Anacetrapib distributes into adipocyte lipid droplet

Corresponding Author: Douglas G. Johns, PhD, FAHA

Department of Translational Pharmacology

Merck &Co., Inc.

PO Box 2000

RY34-A500

Rahway, NJ 07065-0900

Phone: 732-594-7231

Email: douglas.johns@merck.com

# of text pages: 22

# of tables: 0

# of figures: 5

# of references: 21

# of words:

Abstract: 232

Introduction: 401

Discussion: 837

Nonstandard abbreviations

CETP – cholesteryl ester transfer protein

HDL – high density lipoprotein

LDL – low density lipoprotein

VLDL – very low density lipoprotein

ABSTRACT

Anacetrapib is an inhibitor of cholesteryl ester transfer protein (CETP), associated with reduction in LDL-cholesterol and increase in HDL-cholesterol in hypercholesterolemic patients. Anacetrapib was not taken forward into filing/registration as a new drug for coronary artery diease, despite observation of a ~9% reduction in cardiovascular risk in a large phase III cardiovascular outcomes trial (REVEAL). Anacetrapib displayed no adverse effects throughout extensive preclinical safety evaluation, and no major safety signals were observed in clinical trials studying anacetrapib, including REVEAL. However, anacetrapib demonstrated a long terminal half-life in all species, thought to be due, in part, to distribution into adipose tissue. We sought to understand the dependence of anacetrapib's long half-life on adipose tissue, and to explore potential mechanisms which might contribute to the phenomenon. In mice, anacetrapib localized primarily to the lipid droplet of adipocytes in white adipose tissue and in vitro, anacetrapib entry into cultured human adipocytes was dependent upon the presence of a mature adipocyte and lipid droplet, but did not require active transport. In vivo, the entry of anacetrapib into adipose tissue did not require lipase activity, as the distribution of anacetrapib into adipose was-not affected by systemic lipase inhibition using poloaxamer-407, a systemic lipase inhibitor. The data from these studies support the notion that entry of anacetrapib into adipose tissue/lipid droplet does not require active transport or by mobilization and entry of fat into adipose via lipolysis.

INTRODUCTION

Agents that inhibit cholesteryl ester transfer protein (CETP) prevent the exchange of neutral lipid between high, low and very low density lipoproteins (HDL, LDL, VLDL, respectively). The resultant effects of CETP inhibitors on the distribution of cholesterol amongst these lipoproteins, notably increases in HDL-C and decreases in LDL-C, led to their development as drugs that could potentially reduce cardiovascular risk. Across several clinical studies, anacetrapib, a potent inhibitor of CETP, reduced LDL-C and raised HDL-C in normal healthy volunteers and in hypercholesterolemic patients at high risk of cardiovascular disease (CVD) on a background of statin therapy. In a large phase 3 cardiovascular outcomes trial (REVEAL), treatment of patients with atherosclerotic vascular disease with anacetrapib for a mean duration of 4 years led to a relative reduction of ~9% compared to placebo in the primary composite outcome of heart attack, coronary revascularization procedure, or death from coronary heart disease, an effect that appeared to be driven by a reduction in non-HDL-C (Bowman et al., 2017). Despite this reduction in cardiovascular risk, however, a decision was made based on a comprehensive evaluation of the clinical profile of anacetrapib, to not proceed with regulatory filings (Merck & Co. press release, October 11, 2017).

Anacetrapib displays a long terminal half-life in preclinical species and in humans (Gotto et al., 2014; Hartmann et al., 2016). In an extension of a phase 3 clinical safety study (DEFINE), where patients were treated with anacetrapib for 18 months, low levels of anacetrapib in the range of approximately 50 nM were detectable in plasma 2.5-4 years after cessation of dosing (Gotto et al., 2014). We previously reported that in mice treated with anacetrapib for 6 weeks, anacetrapib levels increased in white and brown adipose tissue, and during 35 weeks after cessation of dosing, levels of anacetrapib in white adipose tissue remained relatively unchanged (Hartmann et

al., 2016). Given the lipophilicity of anacetrapib (LogD 7.1), one possibility for the long elimination phase from plasma is that adipose tissue serves as a large depot in the body from which anacetrapib can slowly exit to the plasma compartment, however the mechanisms behind the preferential distribution of anacetrapib into adipose have not been characterized

The purpose of the studies described herein is to further our understanding of the mechanisms behind anacetrapib distribution into adipose. We utilized mice to examine the entry and subcellular localization of anacetrapib into adipose in vivo, and human cultured adipocytes to assess active transport mechanisms of entry in vitro. We report that anacetrapib distributes into the lipid droplet of adipocytes through a mechanism that does not involve active transport or dependence upon lipase-dependent mobilization of lipid.

MATERIALS AND METHODS

Animals

All testing protocols described below were carried out in accordance with the Guide for the Care and Use of Laboratory Animals as adopted and promulgated by the U.S. National Institutes of Health, were approved by the Merck Research Laboratories Institutional Animals Care and Use Committee in Rahway, NJ, and adhered to the PHS policy on Humane Care and Use of Laboratory Animals. Mice were maintained in a 12 h/12 h light–dark cycle with free access to food and water, in group housing conditions in a temperature controlled environment (22°C). Male wild type C57BL/6 mice (WT) used for adipose and plasma pharmacokinetics and adipocyte localization experiments were obtained from Taconic Farms, Inc. (Germantown, NY). Mice were maintained on regular chow (Teklad, 7012, 5% dietary fat; 3.75 kcal/g, Madison, WI). Mice were 12-16 weeks of age at the time experiments were performed.

Anacetrapib pharmacokinetics

To understand the acute (24 hr) vs longer-term time-course of anacetrapib deposition into adipose tissue, male C57BL/6 mice (N=33) were treated with anacetrapib (100 mg/kg/day, oral gavage, dosed as a suspension in 0.5% methycellulose) for 28 days. N=3 mice were euthanized (CO2 asphyxiation followed by cardiac puncture) and blood/tissues collected at the following time points: 0.5, 1, 2, 6, 24 hr following single dose; day 3, 7, 10, 14, 21 28 during once-daily dosing (collection occurred 24 hr after the previous day's dose). Anacetrapib levels in plasma and adipose tissue were determined as described in Hartmann et al. (Hartmann et al., 2016).

Anacetrapib localization in mouse adipose tissue

For determination of subcellular localization of anacetrapib, radiolabeled anacetrapib was prepared by the Radiolabeled Synthesis Group at Merck Research Laboratories in Rahway, NJ. This was a preparation of [1-^{14}C-propane]-2-yl-anacetrapib, with the ^{14}C group on the isopropyl moiety as previously described (Kuethe et al., 2013) with specific activity 0.08932 mCi/mg; 0.3204 mCi/ml; HPLC purity: ^{14}C content= 99.64%, and is referred hereafter as "[^{14}C]-anacetrapib."

For dosing of radiolabeled anacetrapib in mice, cold anacetrapib was initially prepared in Imwitor:Tween-80 (1:1, w:w) in a starting concentration of 10 mg/ml, and sonicated. To make enough solution for 10 mice, 0.44 ml of ^{14}C-anacetrapib in EtOH was added slowly to 0.4 ml of cold anacetrapib solution, under continuous stirring. This preparation was then slowly (under continuous stirring) diluted with 1.16 ml of water (final cold anacetrapib concentration was 2 mg/mL, ^{14}C-anacetrapib was 70 uCi/ml), vortexed and sonicated for 5 min. A stable emulsion was obtained. Mice were dosed via oral gavage at 5 ml/kg. Mice (average weight of 28 grams) received a total dose of 10 uCi/mouse.

Twenty-four hours after dosing, mice were euthanized by CO_2 asphyxiation. Epididymal white adipose tissue was collected and pooled (n=8 mice). Adipocytes were isolated and subcellular fractionation was performed as described by Yu et al. and Bourez et al. (Yu et al., 2000; Bourez et al., 2012). Briefly, adipose tissue was minced and digested with collagenase (1mg/mL in Krebs-Henseleit Buffer supplemented with 2% BSA) for one hour at 37°C. The resulting suspension was then filtered through a 100 μm mesh cell strainer and subjected to a series of washes. The floating fat layer containing the isolated adipocytes was collected and resuspended in disruption buffer (25 mM Tris-HCl, 100mM KCl, 1mM EDTA, 5mM EGTA, pH 7.4 supplemented with protease inhibitors). Cells were disrupted by nitrogen cavitation at 450 psi for

15 minutes at 4°C after which the cavitate was collected dropwise and transferred to a polyallomer sealable tube. Nuclei were pelleted by spinning at 1500g for 10 minutes. The top fat layer was removed via a tube slicer and the infranatant was collected away from the nuclei pellet. The fat layer and the infranatant were each mixed with an equal volume of disruption buffer containing 1.08M sucrose and then overlaid sequentially with 2mL each of 270mM sucrose buffer, 135mM sucrose buffer and Top Solution (25mM Tris-HCl, 1mM EDTA, 1mM EGTA, pH7.4). Following centrifugation for one hour at 150,000g in a SW 41 Ti rotor, 8 1.5mL fractions were collected from top to bottom. The resulting microsomal pellet, as well as the nuclei pellet collected earlier, were washed and resuspended in 1.5mL Top Solution by sonication, 1.0 mL of which was added to Ultima Gold scintillation cocktail (Perkin Elmer, Waltham, MA) and counted on a scintillation counter.

Immunoblotting

Protein from cellular fractions was concentrated and collected from spin columns (Amicon Centrifugal Filter Device, Millipore) using manufacturer's instructions. Proteins were isolated from buoyant lipid fractions using methods as described by Brasaemle and Wolins (Brasaemle and Wolins, 2006) and resultant pellet was resuspended in 2X SDS sample buffer and incubated at 60°C for 4-6 hours in a sonicating water bath. 5 μg of protein per fraction were run under denaturing conditions on 12% Tris-Glycine gels. After transfer to nitrocellulose membranes, blots were blocked with Odyssey Blocking Buffer (LI-COR) for one hour at room temperature. Membranes were probed with primary antibodies against either perilipin (Fitzgerald Industries International; Acton, MA) or GLUT4 (Abcam; Cambridge, MA) diluted in blocking buffer with 0.2% Tween 20. Blots were washed in PBS with 0.1% Tween 20 three times for 5 minutes prior to incubation with the appropriate IRDye secondary antibody (LI-COR; Lincoln, NE) diluted in

blocking buffer with 0.2% Tween 20 and 0.1% SDS. After another round of washes, protein signals were visualized and the intensities of the bands were measured using Odyssey Imager (LI-COR; Lincoln, NE). Intensity readings were converted to percentage of total intensity in graphical representations.

Cell culture experiments

Human preadipocytes (hPADs, pooled as a mix of unknown gender) were obtained from Cell Applications Inc. (San Diego, CA). Preadipocytes were thawed from frozen stocks (received frozen stocks at passage 5-10) and plated into 24 well plates for differentiation at ~90,000 cells/well. Cells were cultured in growth medium, which contains DMEM/F12, 3.3 nM biotin, 1.7 mM pantothenate, and 10% fetal bovine serum. Adipocyte differentiation was initiated by placing the cells in Quick Differentiation Medium, composed of DMEM/F12, 3.3mM biotin, 1.7 mM pantothenate, 0.01 mg/mL transferrin, 20 nM insulin, 100 nM cortisol, 0.2 mM T3, 25 mM dexamethasome, 250 μM 3-Isobutyl-1-methylxanthine (IBMX), and 2 μM rosiglitazone. After four days of differentiation induction, cells were cultured in 3FC medium, which contains DMEM/F12, 3.3 mM biotin, 1.7 mM pantothenate, 0.01 mg/mL transferrin, 20 mM insulin, 100 mM cortisol, and 0.2 mM T3 for up to an additional 10 days. Cells were typically studied between 10-14 days post differentiation with 70~90% fully differentiated. For experiments involving ATP depletion, on the day of the experiment cells were pre-treated for 1-hr with either control media (serum free culture media containing 0.2% BSA), or serum- and glucose-free media supplemented with 0.2% BSA and ATP depletion agents (1 μM rotenone plus 1 μM antimycin A and 10 mM 2-deoxy-D-glucose) (Wick et al., 1957; Palmer et al., 1968; Giudicelli et al., 1977; Bashan et al., 1993; Kim et al., 1999). Concentrations of ATP depletion agents were determined as the minimum concentrations, in combination, that blocked radiolabeled adenosine

uptake (see below) in adipocytes without impacting cell viability during the treatment and uptake protocol. Following ATP depletion, [2,8-^{3}H]-adenosine from American Radiolabeled Chemicals Inc, and [^{14}C]-labeled anacetrapib were utilized to investigate transporter mediated substrate uptake. For adenosine uptake, final concentration of 2 μCi/mL of [2,8-^{3}H]-adenosine mixed with 10 μM of non-labeled adenosine was used for uptake experiments. A specific adenosine transporter inhibitor, S-(4-Nitrobenzyl)-6-thioinosine (NBMPR, Sigma-Aldrich, St. Louis, MO)(Aronow et al., 1985) at 0.1 μM, was used as a positive control for adenosine uptake blockade. A final concentration of 1.44 μCi/mL of [^{14}C]-anacetrapib mixed with 10 μM of non-labeled anacetrapib was used for anacetrapib uptake experiments. In these experiments, cells were treated with radiolabeled anacetrapib (triplicate replicate wells in a 24-well plate), media was collected, and cells were washed three times with PBS followed by lysis with 0.5 mL of 0.1N NaOH. The lysate and media were stored in -20°C until ready for analysis. 300 μl of media and lysate were counted on a liquid scintillation counter in 3 mL of Ultima Gold (Perkin Elmer, Waltham, MA). In some experiments, uptake of radiolabeled anacetrapib was compared amongst mature adipocytes, pre-adipocytes and a non-adipocyte cell line (CHO-K1; ThermoFisher, cultured in DMEM/F12 + 10% fetal bovine serum).

Effects of lipase inhibition on anacetrapib plasma and adipose pharmacokinetics in vivo

To examine the role of lipase in the localization of anacetrapib to adipose tissue, male C57BL/6 mice were dosed with either PBS or poloxamer 407 (P-407) to inhibit hepatic, endothelial, and lipoprotein-associated lipases (Wasan et al., 2003; Millar et al., 2005; Johnston et al., 2010) (1000 mg/kg, intraperitoneal injection) 1 hour before they were orally dosed with anacetrapib at 100 mg/kg. N=4 mice were euthanized as described above and plasma and epididymal white

adipose were collected for measurement of anacetrapib concentration in plasma and tissue, and measurement of plasma lipids. Plasma triglyceride and total cholesterol were measured using triglyceride and total cholesterol kits from Wako Diagnostics (Mountain View, CA), according to manufacturer's instructions.

Statistical analysis

For experiments involving two factors, two–way ANOVA followed by Sidak multiple comparison tests was performed (GraphPad Software, Inc., San Diego, CA). For individual pair-wise comparisons, Student's t-test was performed (GraphPad Software, Inc.)

Chemicals and compounds

Reagents were obtained from commercial sources as indicated. Anacetrapib and [^{14}C]-anacetrapib were synthesized and prepared in Medicinal Chemistry Department at Merck & Co., Inc. (Rahway, NJ).

RESULTS

Anacetrapib localizes to the lipid droplet of adipocytes

Following oral dosing of anacetrapib in mice (100 mg/kg), levels of anacetrapib reached a maximum of approximately 10 μM in white adipose tissue and 4 μM in plasma after a single dose (Figure 1, panel A), but dropped to approximately 3 μM and 0.1 μM by 24 hours, respectively. During 28 days of dosing, levels of anacetrapib in white adipose tissue remained at approximately 2 μM, and plasma levels remained between 0.1 and 0.2 μM (Figure 1, panel B). Because anacetrapib entered adipose tissue readily within 24 hr, acute dosing could be used to

examine localization of anacetrapib in adipose tissue using radiolabeled compound. A separate group of mice were treated with [^{14}C]-Anacetrapib to track the location of anacetrapib-associated radioactivity in adipose tissue. Following density-gradient ultracentrifugation of adipose tissue, the lipid droplet-associated protein perilipin (Brasaemle, 2007) was used to confirm the identity/purity of the fraction containing the lipid droplet (Figure 2, panel A). The majority of [^{14}C]-anacetrapib-associated radioactivity colocalized in the same fraction as perilipin, suggesting that the site of anacetrapib deposition in adipose tissue is the lipid droplet (Figure 2, panel B).

Entry of anacetrapib into cultured human adipocytes is facilitated by presence of lipid droplet, but does not require active transport.

To further understand mechanisms of entry of anacetrapib into adipocytes, cultured human adipocytes were differentiated from preadipocytes into mature adipocytes as described in Materials and Methods, and uptake of [^{14}C]-anacetrapib was examined before and after differentiation. Maturation of adipocytes was confirmed by the presence of a lipid droplet. Following 48 hr incubation with radiolabeled anacetrapib, intracellular levels of [^{14}C]-anacetrapib-associated radioactivity were greater in mature/differentiated adipocytes compared to pre-adipocytes (Figure 3), suggesting the lipid droplet increases anacetrapib partitioning and further supporting the lipid droplet as the primary site of anacetrapib deposition. Uptake of radiolabeled anacetrapib was also compared between mature adipocytes and CHO cells, which served as a non-adipocyte cell type. Intracellular levels of radiolabeled anacetrapib were significantly greater in mature adipocytes compared to CHO cells (Figure 3).

To determine whether the uptake of anacetrapib requires active transport, cells were treated with a cocktail of compounds to inhibit synthesis of ATP (NaN_3, rotenone, antimycin A and 2-deoxyglucose). Blockade of active transport was confirmed by the inhibition of adenosine uptake (Figure 4, panel A). Under the same conditions which blocked adenosine uptake, anacetrapib uptake was unaffected (Figure 4, panel B), indicating that the entry of anacetrapib into adipocytes does not require active transport.

Mechanism of anacetrapib entry into adipose is independent of lipase activity

Given that anacetrapib-associated radioactivity was found to primarily localize to the lipid droplet of adipocytes, experiments were performed to determine if mobilization of fatty acids by lipase-activity plays a role in the initial uptake of anacetrapib into adipose tissue, WT mice were treated with a single dose of anacetrapib in the presence and absence of 1000 mg/kg Poloxamer 407 (P-407) to inhibit hepatic, endothelial, and lipoprotein-associated lipases (13-15). P-407 treatment was associated with a large increase in plasma lipids (Figure 5, panel A), consistent with inhibition of lipase and subsequent prevention of fatty acid mobilization and transfer from blood to tissues. Plasma levels of anacetrapib were significantly increased in P-407-treated mice compared to PBS-treated controls (Figure 5, panel B), and plasma anacetrapib levels followed a similar time-course as plasma triglyceride. Despite this large difference in plasma anacetrapib levels between P407- and PBS-treated mice, levels of anacetrapib in adipose tissue were not different between each treatment group, except at the 0.5 and 1hr time points, where adipose levels of anacetrapib were actually higher in P407-treated animals (Figure 5, panel B).

DISCUSSION

The long terminal half-life of anacetrapib is thought to be due prolonged retention in adipose tissue. We previously reported sustained levels of anacetrapib in white adipose tissue for at least 35 weeks after cessation of dosing in mice (Hartmann et al., 2016), and in humans, low levels of anacetrapib persist in plasma years after dosing (Gotto et al., 2014). A recent report by Krishna et al (Krishna et al., 2017) described the accumulation of anacetrapib during dosing and persistence of anacetrapib in adipose tissue after dosing in human subjects, similar to what was observed in mice. Taken together, these observations support the notion that retention and very slow elimination from adipose tissue explains both the long terminal plasma half-life and the persistence of anacetrapib levels in plasma years after dosing is stopped.

In the current study, anacetrapib entered adipose tissue quickly in mice, reaching a maximum concentration (~10 μM) approximately 2 hours following a single 100 mg/kg dose, falling to a trough level at 24 hours which remained stable for the 28 day dosing period. Harvesting and fractionating white adipose tissue from [^{14}C]-labeled anacetrapib-treated mice suggested that anacetrapib resided predominantly in the lipid droplet, evidenced by colocalization of anacetrapib-associated radioactivity with perilipin, a protein marker which is present in the lipid droplet fraction. Furthermore, in cultured cells, the accumulation of anacetrapib-associated radioactivitywas greatest in cells containing a mature lipid droplet (i.e. human differentiated adipocytes), compared to undifferentiated/pre-adipocytes or CHO cells, which do not contain a lipid storage vacuole. The preference of anacetrapib for neutral lipid is not unexpected, given that anacetrapib is a neutral molecule, and its lipid partition coefficient (log D) is approximately 7.1, a value associated with high lipophilicity (Krishna et al., 2017). However, the mechanism by which anacetrapib enters the adipocyte is unclear. It is important to note that due to the

location of the radiolabel on [^{14}C]-anacetrapib the radioactivity measured in the subcellular localization and cultured adipocyte experiments may not represent 100% anacetrapib as a parent molecule, and could include radiolabeled metabolites of anacetrapib. Given that the unlabeled anacetrapib which accumulates in adipose tissue to micromolar concentrations, as reported in Figure 1, is measured as "parent" anacetrapib, the majority of radioactivity measured in the radiolabeled anacetrapib experiments is assumed to be parent. However, it cannot be ruled out that a proportion of the radioactivity reported in the subcellular lipid droplet fraction, and in the cell lysate of cultured cells, could be metabolites of anacetrapib.

Krishna et al (Krishna et al., 2017) reported that the majority of plasma anacetrapib in humans is carried in lipoproteins. While some anacetrapib is expected to be bound to CETP in the lipoprotein fraction (specifically high density lipoprotein), as described by Ranalletta et al (Ranalletta et al., 2010), concentrations of plasma/lipoprotein-associated anacetrapib, as described by Krishna et al., are higher than reported plasma concentrations of CETP in humans (~25nM)(Marcel et al, 1990). Therefore it is likely that lipoprotein-associated anacetrapib (not bound to CETP) is carried in the neutral lipid core. The WT mice used in this study lack CETP, and presumably, the anacetrapib carried in the lipoprotein fraction is located in the neutral lipid core of the particle. The use of CETP-deficient/WT mice to study anacetrapib distribution into adipose tissue is justified by our previous report that the lack of CETP has no effect on the ability of anacetrapib to accumulate into adipose tissue (Hartmann et al., 2016).

If lipoproteins "deliver" anacetrapib to adipose tissue, then mechanisms responsible for mobilization and transport of fatty acids into adipose for storage (i.e. active transport, lipase-mediated lipolysis) could also be responsible for transport of anacetrapib into adipocytes. The cocktail of rotenone, antimycin A and 2-Deoxyglucose, was used to inhibit ATP production from

mitochondrial electron transport/oxidative phosphorylation, and glycolysis (Wick et al., 1957; Palmer et al., 1968; Giudicelli et al., 1977; Bashan et al., 1993; Kim et al., 1999), at the minimum concentrations found to maximally block adenosine uptake into adipocytes, a process dependent upon ATP-mediated active transport (Molina-Arcas et al., 2009; Gray et al., 2004). Active transport blockade had no effect on anacetrapib entry into cells, indicating that anacetrapib must enter these cells via a mechanism independent of ATP. Poloaxamer 407 (P407) inhibits systemic lipase activity in vivo (Wasan et al., 2003; Millar et al., 2005; Johnston et al., 2010), and pretreatment of mice with P407 resulted in a large increase in plasma triglyceride, evidence that lipase-mediated lipolysis (and therefore uptake of lipid) was inhibited. This increase in plasma lipid was accompanied by large increases in plasma anacetrapib, which is consistent with the notion that since lipoproteins are responsible for carrying neutral lipid (i.e. triglyceride, cholesterol ester) in plasma, the capacity of lipoproteins to carry anacetrapib is increased with increased lipoprotein-associated triglyceride, given the high logD of anacetrapib. This observation is also consistent with our previous report in mice, where plasma anacetrapib levels were higher in obese/hyperlipidemic WT mice (diet-induced obesity) compared to lean WT controls (Hartmann et al., 2016). If lipase-mediated lipolysis was involved in the mobilization and entry of anacetrapib into adipose tissue, a reduction in adipose anacetrapib would have been observed. However no reduction in adipose anacetrapib levels was observed. Taken together, these data suggest that anacetrapib does not follow a path into adipose tissue similar to the mechanisms known to mediate fatty acid storage. Candidate mechanisms for anacetrapib entry into adipose tissue include passive diffusion, or holoparticle uptake of lipoproteins via scavenger receptors, however these mechanisms require additional study.

In conclusion, anacetrapib rapidly partitions into adipose tissue and localizes into the lipid droplet component of the adipocyte, via a process independent of active transport or lipase activity. Because lipolysis does not play a role in the mobilization of anacetrapib from lipoprotein, it is interesting to speculate that the reverse process, lipolysis of triglyceride to mobilize fatty acids from adipose to the plasma compartment is also not involved in mobilization of anacetrapib from these deep tissue stores. While additional study is required to identify the precise mechanisms of anacetrapib entry and egress from adipose tissue, the findings from the studies described herein could partially explain the extremely slow elimination of anacetrapib from adipose, and the persistence of anacetrapib in the plasma of patients, years after cessation of dosing.

AUTHORSHIP CONTRIBUTIONS

Participated in research design: Johns, LeVoci, Lu, Wang

Conducted experiments: LeVoci, Krsmanovic, Lu, Xu, Wang, Chen

Contributed new reagents or analytic tools: Xu

Performed data analysis: Johns, LeVoci, Krsmanovic, Lu, Xu, Wang, Chen

Wrote or contributed to the writing of the manuscript: Johns, Lu, Hartmann, Bateman, Blaustein

REFERENCES

Aronow B, Allen K, Patrick J, and Ullman B (1985) Altered nucleoside transporters in mammalian cells selected for resistance to the physiological effects of inhibitors of nucleoside transport. *J Biol Chem* 260:6226-6233.

Bashan N, Burdett E, Gumà A, Sargeant R, Tumiati L, Liu Z, and Klip A (1993) Mechanisms of adaptation of glucose transporters to changes in the oxidative chain of muscle and fat cells. *Am J Physiol* 264:C430-440.

Bourez S, Le Lay S, Van den Daelen C, Louis C, Larondelle Y, Thomé JP, Schneider YJ, Dugail I, and Debier C (2012) Accumulation of polychlorinated biphenyls in adipocytes: selective targeting to lipid droplets and role of caveolin-1. *PLoS One* 7:e31834.

Bowman L, Hopewell JC, Chen F, Wallendszus K, Stevens W, Collins R, Wiviott SD, Cannon CP, Braunwald E, Sammons E, and Landray MJ (2017) HPS3/TIMI55-REVEAL Collaborative Group. Effects of anacetrapib in patients with atherosclerotic vascular disease. *N Engl J Med* 377:1217-1227.

Brasaemle DL and Wolins NE (2006) Isolation of lipid droplets from cells by density gradient centrifugation. *Curr Proto Cell Biol* Chapter 3:Unit 3.15.

Brasaemle DL (2007) The perilipin family of structural lipid droplet proteins: stabilization of lipid droplets and control of lipolysis. *J Lipid Res* 48:2547-2559.

Giudicelli Y, Pecquery R, Provin D, Agli B, and Nordmann R (1977) Regulation of lipolysis and cyclic AMP synthesis through energy supply in isolated human fat cells. *Biochim Biophys Acta* 486:385-398.

Gotto AM Jr, Cannon CP, Li XS, Vaidya S, Kher U, Brinton EA, Davidson M, Moon JE, Shah S, Dansky HM, Mitchel Y, and Barter P (2014) DEFINE Investigators. Evaluation of lipids, drug concentration, and safety parameters following cessation of treatment with the cholesteryl ester transfer protein inhibitor anacetrapib in patients with or at high risk for coronary heart disease. *Am J Cardiol* 113:76-83.

Gray JH, Owen RP, and Giacomini KM (2004) The concentrative nucleoside transporter family, SLC28. *Pflugers Archiv* 447:728-734.

Hartmann G, Kumar S, Johns D, Gheyas F, Gutstein D, Shen X, Burton A, Lederman H, Lutz R, Jackson T, Chavez-Eng C, and Mitra K (2016) Disposition into Adipose Tissue Determines Accumulation and Elimination Kinetics of the Cholesteryl Ester Transfer Protein Inhibitor Anacetrapib in Mice. *Drug Metab Dispos* 44:428-434.

Johnston TP (2010) Poloxamer 407 as a general lipase inhibitor: its implications in lipid metabolism and atheroma formation in C57BL/6 mice. *J Pharm Pharmacol* 62:1807-1812.

Kim H, Esser L, Hossain MB, Xia D, Yu C, Rizo J, van der Helm D, and Deisenhofer J (1999) Structure of antimycin A1, a specific electron transfer inhibitor of ubiquinol−cytochrome-c oxidoreductase. *J Am Chem Soc* 121:4902–4903.

Krishna R, Gheyas F, Liu Y, Hagen DR, Walker B, Chawla A, Cote J, Blaustein RO, and Gutstein DE (2017) Chronic administration of anacetrapib is associated with accumulation in adipose and slow elimination. *Clin Pharmacol Ther* 102:832-840.

Kuethe, JT, Soli, ED, Royster, P, Quinn, CA. (2013) Synthesis of stable isotope labeled anacetrapib, its major metabolites and [^{14}C]anacetrapib. *J Label Compd Radiopharm* 56:600-608.

Marcel, YL, McPherson R, Hogue M, Czarnecka H, Zawadzki Z, Weech PK, Whitlock ME, Tall AR, and Milne RW (1990) Distribution and concentration of cholesteryl ester transfer protein in plasma of normolipemic subjects. *J Clin Invest* 85:10-17.

Millar JS, Cromley DA, McCoy MG, Rader DJ, and Billheimer JT (2005) Determining hepatic triglyceride production in mice: comparison of poloxamer 407 with Triton WR-1339. *J Lipid Res* 46:2023-2028.

Molina-Arcas M, Casado FJ, and Pastor-Anglada M (2009) Nucleoside transporter proteins. *Curr Vasc Pharmacol* 7:426-434.

Palmer, G., Horgan, D. J., Tisdale, H., Singer, T. P. and Beinert, H (1968) Studies on the respiratory chain-linked reduced nicotinamide adenine dinucleotide dehydrogenase. XIV. Location of the sites of inhibition of rotenone, barbiturates, and piericidin by means of electron paramagnetic resonance spectroscopy. *J Biol Chem* 243, 844–847.

Ranalletta M, Bierilo KK, Chen Y, Milot D, Chen Q, Tung E, Houde C, Elowe NH, Garcia-Calvo M, Porter G, Eveland S, Frantz-Wattley B, Kavana M, Addona G, Sinclair P, Sparrow C, O'Neill EA, Koblan KS, Sitlani A, Hubbard B, and Fisher TS (2010) Biochemical characterization of cholesteryl ester transfer protein inhibitors. *J Biol Chem* 51:2739-2752.

Wasan KM, Subramanian R, Kwong M, Goldberg IJ, Wright T, and Johnston TP (2003) Poloxamer 407-mediated alterations in the activities of enzymes regulating lipid metabolism in rats. *J Pharm Pharm Sci* 6:189-197.

Wick AN, Drury DR, Nakada HI, and Wolfe JB (1957) Localization of the primary metabolic block produced by 2-deoxyglucose. *J Biol Chem.* 224:963-969.

Yu W, Cassara J, and Weller PF (2000) Phosphatidylinositide 3-kinase localizes to cytoplasmic lipid bodies in human polymorphonuclear leukocytes and other myeloid-derived cells. *Blood* 95:1078-1085.

FOOTNOTES

This research was supported by Merck & Co., Inc., Kenilworth, NJ

Please send reprint requests to:

Douglas G. Johns, PhD, FAHA

Department of Translational Pharmacology

Merck &Co., Inc.

PO Box 2000

RY34-A500

Rahway, NJ 07065-0900

Phone: 732-594-7231

Email: douglas.johns@merck.com

Douglas G. Johns, PhD, FAHA

FIGURE LEGENDS

Figure 1. Pharmacokinetics of anacetrapib in plasma and epididymal white adipose tissue (eWAT) of male C57Bl/6J mice (N=3 mice per time point). Anacetrapib concentrations were determined in plasma and eWAT A) 30 min – 24 hr following a single oral dose (100 mg/kg), and B) for 28 days of once-daily dosing (100 mg/kg, oral gavage), with tissue/plasma collection occurring 24 hr following previous dose (trough). Data points represent mean ± standard error of the mean.

Figure 2. Localization of radiolabeled anacetrapib to the lipid droplet of adipocytes from mice treated with [14C]-anacetrapib (pooled adipose samples from N=8 mice). A) Left panel: Immunoblot of perilipin A and B, showing the greatest signal in the fat fractions, with small amounts located in the microsome and nuclear fraction; Right panel: densitometry of perilipin signal; B) graph depicting radioactivity associated with subcellular fractions of adipose tissue from WT mice treated for 24 hours with 10 μCi of [14C]-anacetrapib (in a dosing solution of cold anacetrapib to deliver 10mg/kg total) , indicating greatest amount of anacetrapib-associated radioactivity occurring in the lipid droplet fraction.

Figure 3. Entry of [^{14}C]-anacetrapib in human cultured adipocytes, compared to pre-adipocytes and non-adipocyte cells (CHO-K1 cells). Cells were treated with 1.44 μCi/mL of [^{14}C]-anacetrapib mixed with 10 μM of non-labeled anacetrapib and cell lysates were counted in a scintillation counter. Anacetrapib-associated radioactivity increased in a time-dependent manner to a greater extent in mature adipocytes (open circles) compared to pre-adipocytes (closed circles) and CHO cells (closed triangles). [a] $P<0.05$ comparing adipocytes to pre-adipocytes;

[b]*P*<0.05 comparing adipocytes to CHO cells. Data points represent mean cpm ± SEM from triplicate replicates from one of three experiments with similar results.

Figure 4. Blockade of active transport does not impair entry of [14C]-anacetrapib into adipocytes. A) Blockade of radiolabeled adenosine transport into adipocytes by 1 μM rotenone, 1 μM antimycin A and 10 mM 2-deoxy-D-glucose (2-DG) confirms active transport blockade under these conditions. S-(4-nitrobenzyl-6-thioinosine), an adenosine transporter antagonist, was used as a positive control for blockade of adenosine uptake. ***P<0.001 vs vehicle for rotenone/antimycin/2-DG treatment; B) Treatment of adipocytes with rotenone/antimycin/2-DG has no effect on time-dependent [^{14}C]-anacetrapib uptake (left panel) or concentration-dependent [^{14}C]-anacetrapib uptake (right panel). *P<0.05 vs control. Data points represent mean cpm ± SEM from one of three independent experiments with similar results.

Figure 5. Lipase inhibition does not impair entry of anacetrapib into adipose tissue in mice. Male WT mice were treated with 100 mg/kg anacetrapib 1 hr after pre-treatment with P407 (1000 mg/kg) and plasma and eWAT collected at various time points over 24 hours. A) plasma triglyceride (TG, left panel) and plasma total cholesterol (TC, right panel) were significantly increased following P407 treatment of mice, compared to PBS control; B) plasma (left panel) and eWAT (right panel) concentrations of anacetrapib following P407 treatment. *P<0.05, **P<0.01, ***P<0.001 vs PBS control. Each data point represents mean ± standard error of the mean from N=3 animals.

DMD Fast Forward. Published on December 19, 2018 as DOI: 10.1124/dmd.118.084525
This article has not been copyedited and formatted. The final version may differ from this version.

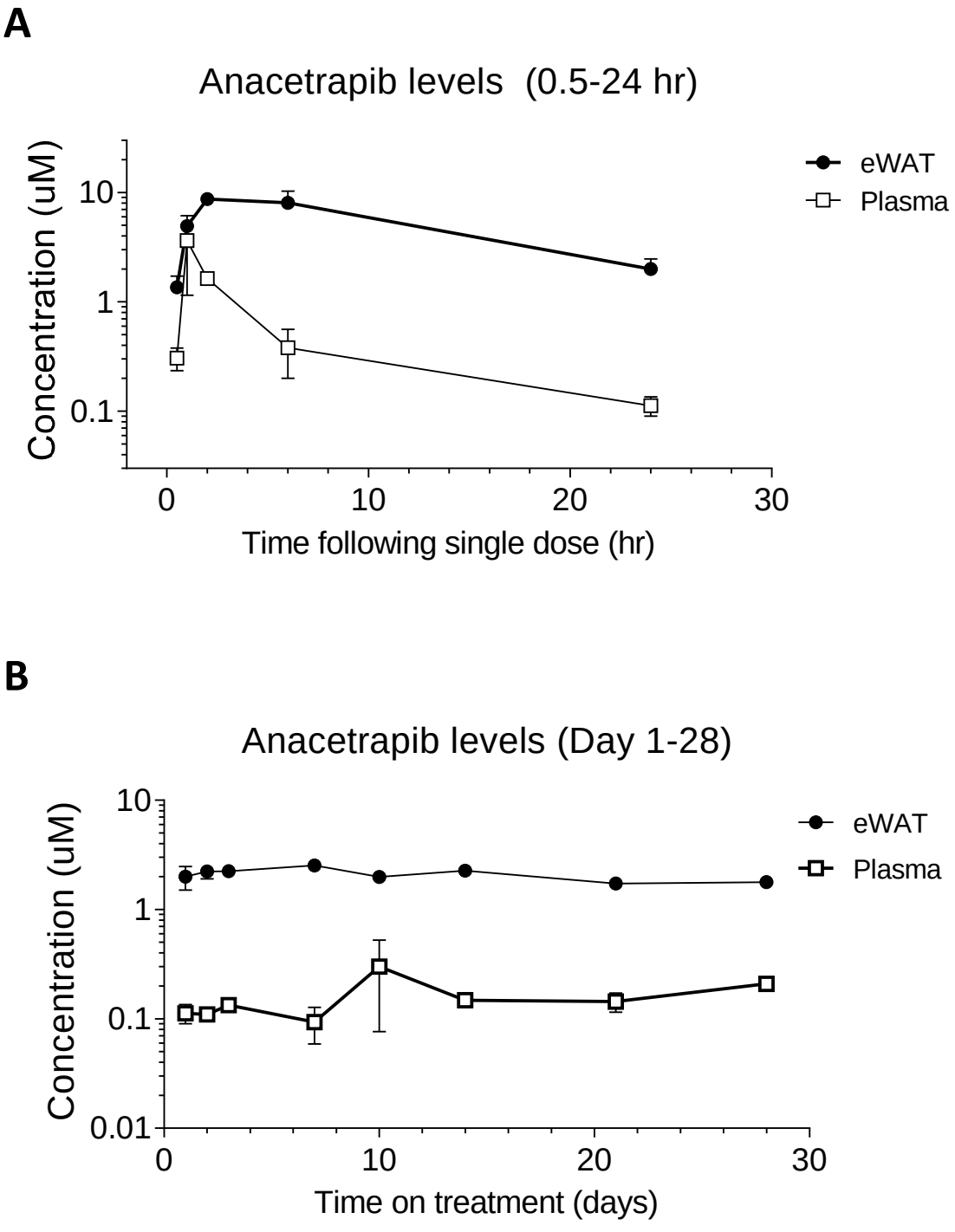

Figure 1.

DMD Fast Forward. Published on December 19, 2018 as DOI: 10.1124/dmd.118.084525
This article has not been copyedited and formatted. The final version may differ from this version.

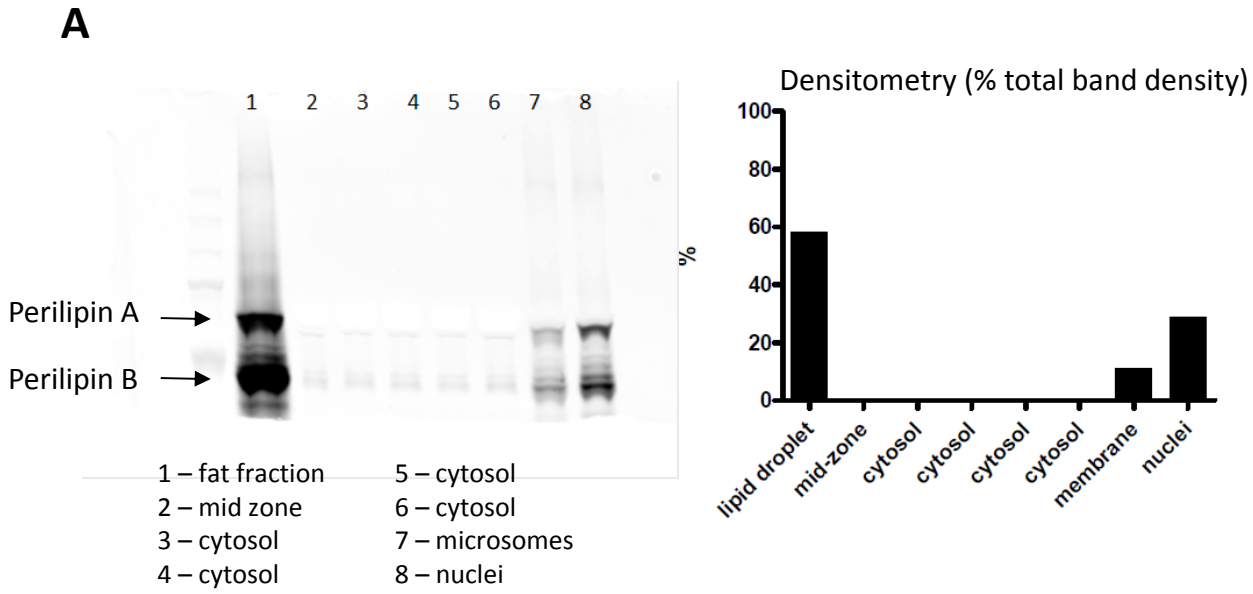

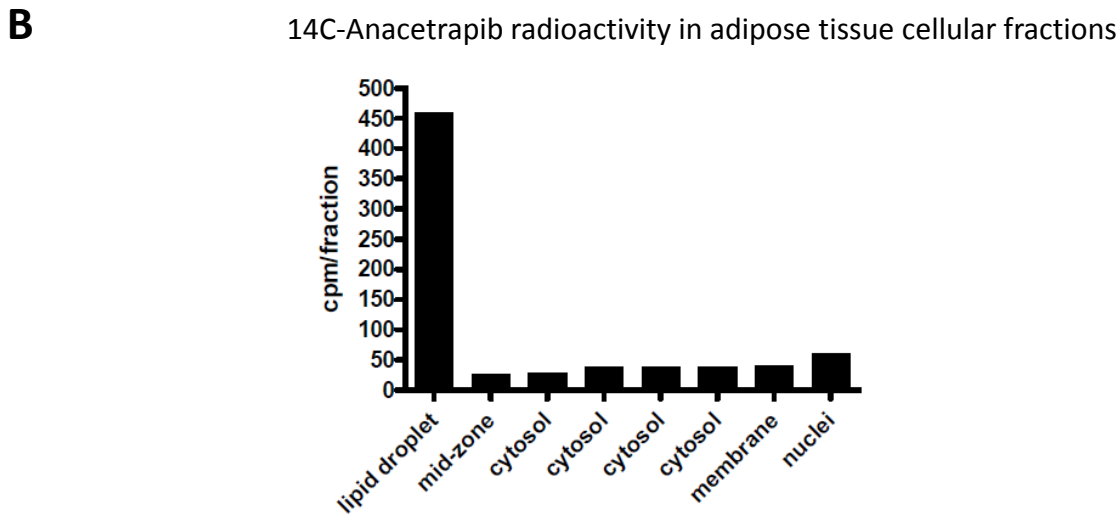

Figure 2.

DMD Fast Forward. Published on December 19, 2018 as DOI: 10.1124/dmd.118.084525
This article has not been copyedited and formatted. The final version may differ from this version.

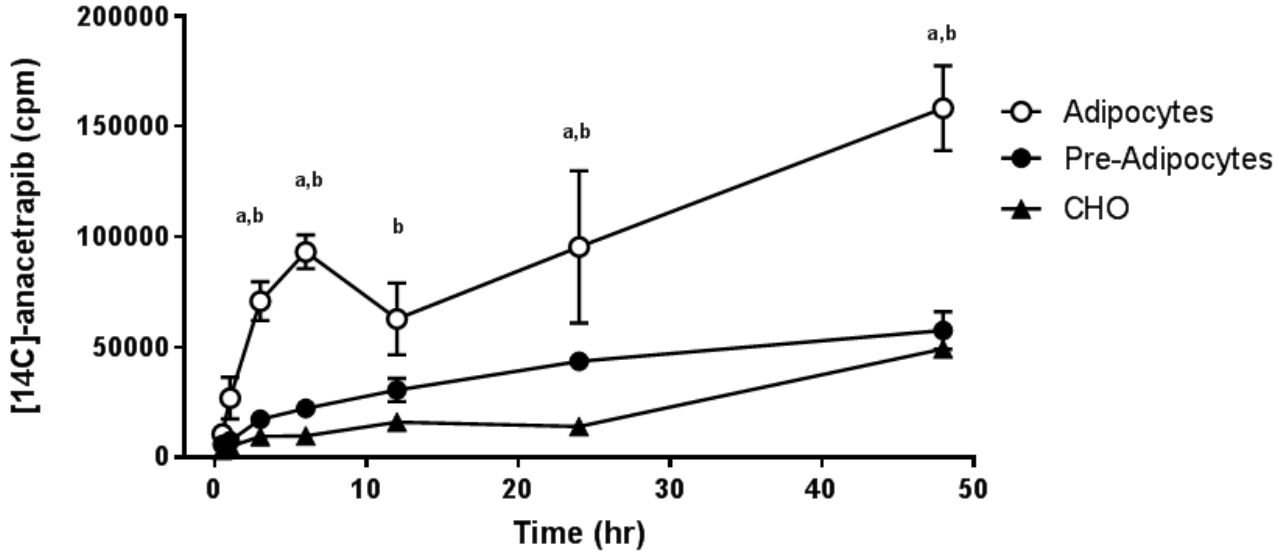

Figure 3.

DMD Fast Forward. Published on December 19, 2018 as DOI: 10.1124/dmd.118.084525
This article has not been copyedited and formatted. The final version may differ from this version.

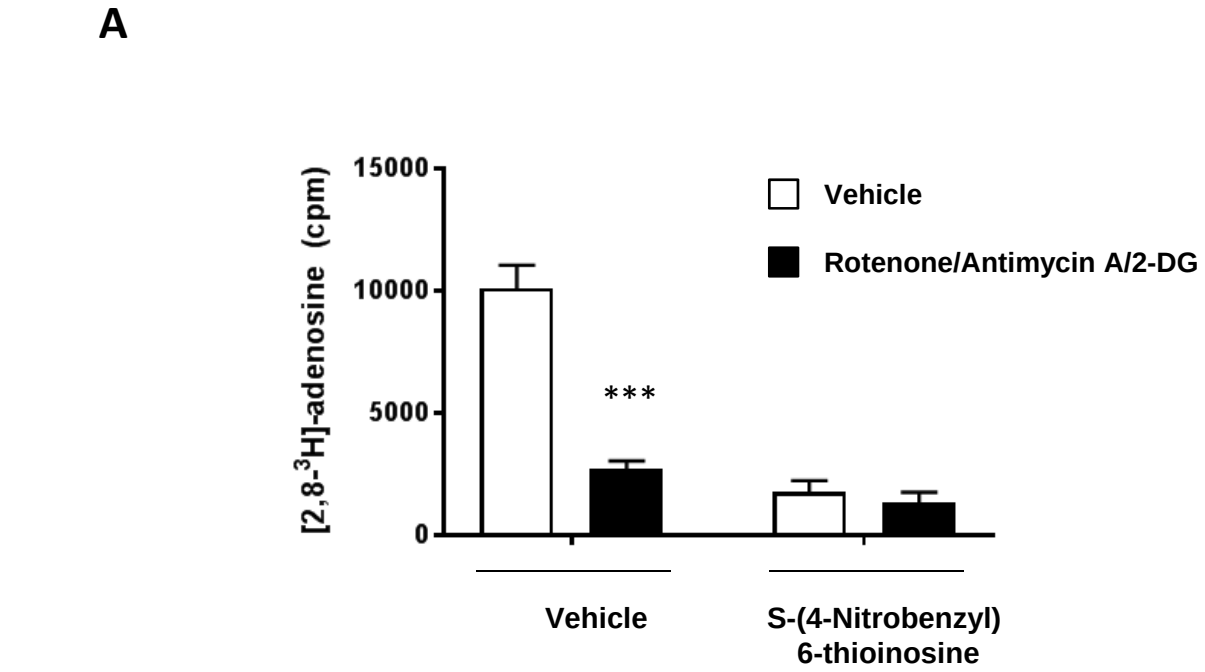

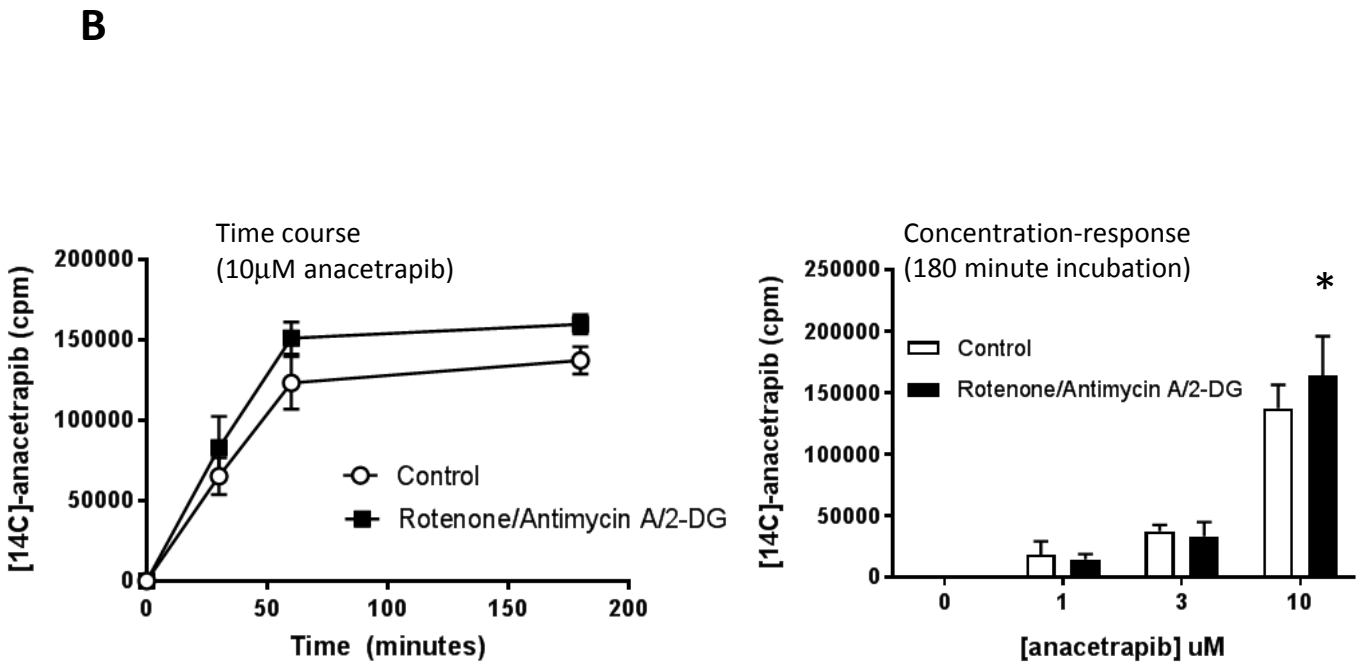

Figure 4.

DMD Fast Forward. Published on December 19, 2018 as DOI: 10.1124/dmd.118.084525
This article has not been copyedited and formatted. The final version may differ from this version.

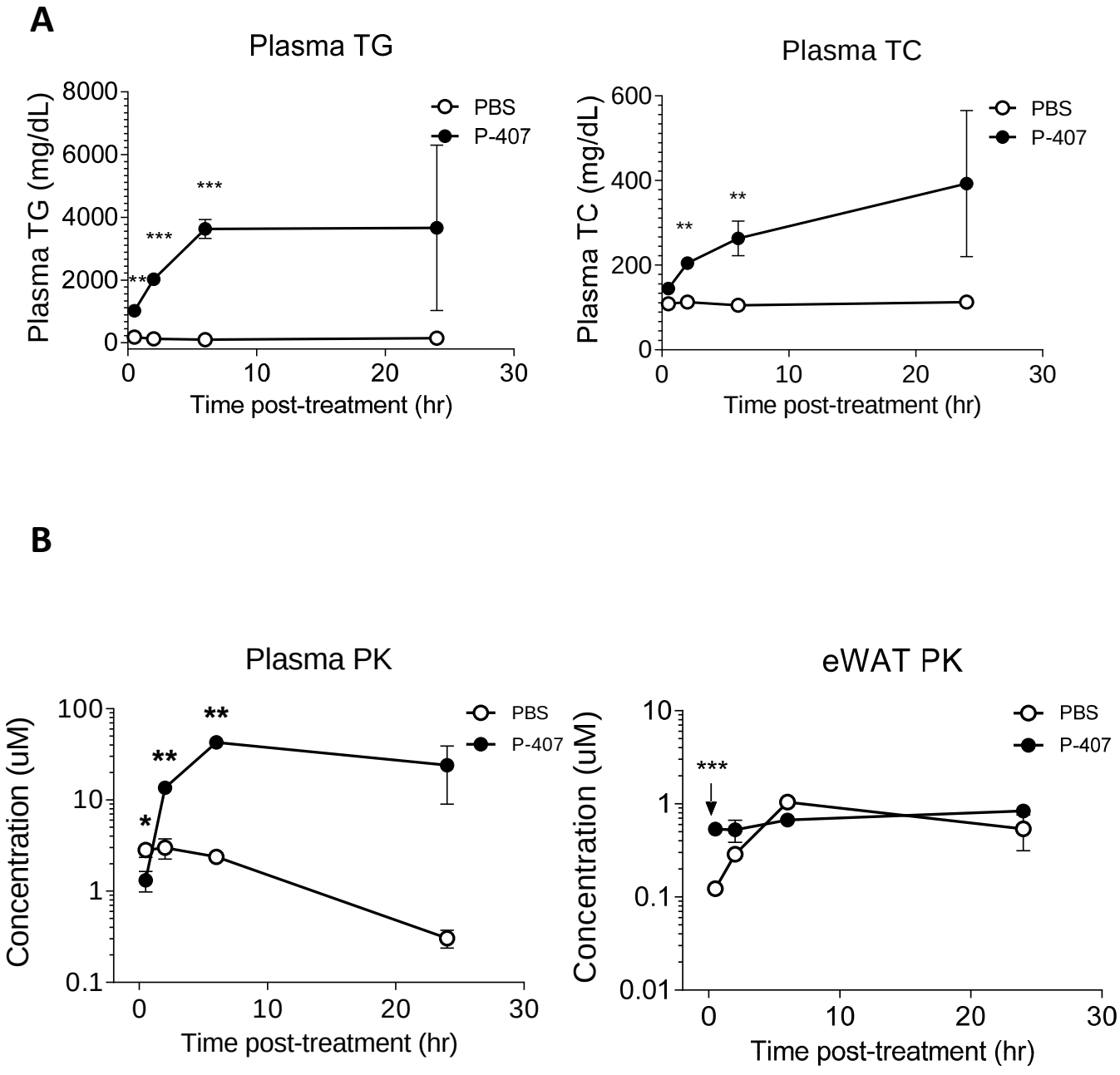

Figure 5